Powder Technology 241 (2013) 174–180

Contents lists available at SciVerse ScienceDirect

Powder Technology

journal homepage: www.elsevier.com/locate/powtec

Periodic flow structures in vertical gas-particle flows

Xiaokang Yan [a,b], William Holloway [a], Sankaran Sundaresan [a,*]

[a] Department of Chemical and Biological Engineering, Princeton University, Princeton, NJ 08544, USA
[b] School of Chemical Engineering, China University of Mining and Technology, Xuzhou 221116, PR China

ARTICLE INFO

Article history:
Received 12 January 2013
Received in revised form 6 March 2013
Accepted 12 March 2013
Available online 18 March 2013

Keywords:
Gas-particle flows
Oscillation
Riser flow
Two-fluid model
Kinetic theory

ABSTRACT

Simulations of kinetic theory based two-fluid model for gas-particle flows in vertical riser segments have been performed. In two-dimensional (2D) simulations of flows in a vertical channel segment and in three-dimensional (3D) simulations of flows in a vertical cylindrical riser segment, periodic boundary conditions were employed in the axial direction. These were supplemented by simpler quasi-one-dimensional (1D) simulations of channel flow and quasi-2D simulations in cylindrical geometry, where it was postulated that the flow variables did not change axially. Both 2D and quasi-1D simulations of channel flow were found to manifest in a robust manner quasi-periodic solutions consisting of laterally traveling waves. Similarly, quasi-2D and 3D simulations of cylindrical riser flow manifested spinning flow states, which in the case of high aspect ratios showed signs of transition to swirling flow states. The period of the oscillating/spinning flow could be captured by a rather simple correlation, whose structure suggests a microscopic origin for the flow structure. The centrifugal force associated with the spin appears to be sufficient to impart an influence on the extent of radial segregation of particles.

1. Introduction

Gas-particle flows in vertical risers manifest persistent meso-scale fluctuations in phase velocities as well as particle volume fractions that span a wide range of length and time scales. Resolving all these fluctuations in industrial scale devices poses formidable computational challenges. To make the simulations computationally affordable, researchers have considered different approaches:

(a) Device-scale steady-state simulations using kinetic-theory based constitutive relation for the particle phase stress and ignoring the influence of meso-scale fluctuations [1,2];
(b) Device-scale transient simulations of two-fluid model equations on relatively coarse grids using either phenomenological or kinetic-theory based constitutive relations for the particle phase stress, neglecting the potential influence of unresolved sub-grid scale fluctuations [3,4];
(c) Device-scale transient simulations of filtered two-fluid model equations on relatively coarse grids using filtered constitutive relations for the fluid-particle drag force and particle phase stress that attempt to incorporate the influence of unresolved sub-grid scale fluctuations [5–8];
(d) Highly-resolved transient simulations of two-fluid model equations in small, highly idealized geometries using either phenomenological or kinetic-theory based constitutive relations for the particle phase stress [9–11].

The first three types of gas-particle flow simulations have generally been aimed at testing if the physical phenomena included in the analysis are sufficient to capture the flow behavior measured experimentally.

In contrast, the fourth kind of simulations has been aimed at understanding the fine structures and their potential influence on the nature of flow. Researchers have simulated unsteady flows in fully periodic domains [9–12]; quasi-one-dimensional (1D) flows assuming that the flow variables depend only on the lateral direction (for channel flow) or radial direction (for flow in cylindrical pipes) and time [13,14]; quasi-two-dimensional (2D) flows assuming that the flow variables depend only on the radial and azimuthal directions (for flow in cylindrical pipes) and time [15]; and unsteady 2D flows in vertical channels and imposing periodic boundary conditions in the axial direction [16]. A natural extension of this type of simulation would consider three-dimensional (3D) flows in (vertical) cylinders, imposing periodic boundary conditions in the axial direction. Such simulations have given insights about the fine structures afforded by the two-fluid models as well as exposed possible coherent structures, which may have been missed in the first three kinds of simulations because of inadequate resolution of the fine scale structures. Quasi-1D simulations of flow in a vertical channel by Benyahia et al. [13,14] revealed coherent structure where the phase volume fraction field settled into quasi-periodic oscillatory pattern whose frequency was in the range of fluctuations seen experimentally. Such oscillatory

* Corresponding author.
E-mail address: sundar@princeton.edu (S. Sundaresan).

0032-5910/$ – see front matter © 2013 Elsevier B.V. All rights reserved.
http://dx.doi.org/10.1016/j.powtec.2013.03.024

flow patterns do not appear to have been documented in device scale studies.

In the present study, we examine this coherent structure in a greater detail. We have studied systematically quasi-1D and quasi-2D simulations in vertical channels and cylinders respectively; these results show that oscillations in quasi-1D channel flow simulations give way to spinning flows in quasi-2D simulations of flows in vertical cylinders. The oscillation frequencies observed for various systems and particle properties can be neatly collapsed into a simple model, which strongly suggest a microscopic physical origin. 2D simulations in channels employing periodic boundary conditions in the axial direction show that the oscillatory pattern transforms to a meandering flow as the length of the simulation domain in the axial direction is increased while fully 3-D simulations in axially periodic vertical cylinder suggest that the spinning mode may transform to spiral flow. In the following sections, we present these results and discuss their implications.

2. Mathematical model

Gas-particle flow in riser segments were simulated in this study using kinetic-theory based two-fluid model [17,18], implemented in the open-domain Multiphase Flow with Inter-phase Exchanges (MFIX) code [19–21]; specifically, version MFIX 2012–1 was used in all the simulations. The two-fluid model, consisting of continuity and momentum equations for the two phases, is summarized below:

$$\frac{\partial(\rho_s\phi_s)}{\partial t}+\nabla\cdot(\rho_s\phi_s\mathbf{v})=0 \tag{1}$$

$$\frac{\partial\left(\rho_g(1-\phi_s)\right)}{\partial t}+\nabla\cdot\left(\rho_g(1-\phi_s)\mathbf{u}\right)=0 \tag{2}$$

$$\frac{\partial(\rho_s\phi_s\mathbf{v})}{\partial t}+\nabla\cdot(\rho_s\phi_s\mathbf{vv})=-\nabla\cdot\sigma_s-\phi_s\nabla\cdot\sigma_g+f+\rho_s\phi_s\mathbf{g} \tag{3}$$

$$\frac{\partial\left(\rho_g(1-\phi_s)\mathbf{u}\right)}{\partial t}+\nabla\cdot\left(\rho_g(1-\phi_s)\mathbf{uu}\right)=-(1-\phi_s)\nabla\cdot\sigma_g-f+\rho_g(1-\phi_s)\mathbf{g} \tag{4}$$

These are supplemented by the granular energy balance equation:

$$\frac{\partial(\frac{3}{2}\rho_s\phi_sT)}{\partial t}+\nabla\cdot\left(\frac{3}{2}\rho_s\phi_sT\mathbf{v}\right)=-\nabla\cdot\mathbf{q}-\sigma_\mathbf{s}:\nabla\mathbf{v}+\Gamma_{\text{slip}}-\text{J}_{\text{coll}}-\text{J}_{\text{vis}} \tag{5}$$

The Wen and Yu [22] model for the fluid–particle interaction force, **f**, and the kinetic theory closures for the stresses and the various terms appearing in the granular energy balance equation used in our simulations can be found in ref. [9,10]. They are not repeated here for the sake of brevity.

At the riser walls, unless specified otherwise, free-slip boundary condition for the gas phase, and the momentum and granular energy conditions proposed by Johnson and Jackson [23] for the particle phase were employed in our simulations. A few simulations were also performed using no-slip boundary conditions for the particle phase. As periodic boundary conditions apply in the vertical direction, the average volume fraction of particles in the simulation domain is invariant with time. Instead of specifying the average pressure gradient in the vertical direction, the cross-sectional average gas mass flux is held constant during the simulations. This is an option available in MFIX (and used by Benyahia et al. [13,14]), where the mean pressure gradient in the vertical direction is adjusted as a function of time to control the average gas mass flux. Simulations were started from slightly inhomogeneous initial conditions and allowed to develop into a periodic, quasi-periodic or fluctuating (but statistically steady) state.

3. Results and discussion

3.1. Flows in vertical channels

Fig. 1 shows gray-scale plots of gas volume fraction field at three successive times within the statistical steady state obtained in a 2D channel (slit) flow simulation. When the particle-rich region is close to a wall, a nearly columnar structure is clearly seen; however, when this structure is traveling from one wall towards the other, the columnar structure is broken up first and formed again. Fig. 2 shows the average volume fraction of gas in one-half of the channel as a function of time; quasi-periodic oscillation is readily evident. It can be inferred from snapshots such as those shown in Fig. 1 that a wave moves from one wall towards the other, bounces off the wall and travels in the opposite direction in a nearly periodic fashion. By sampling the results over 100 s of simulation time, the average period of oscillation was estimated, which in this case was 4.7 s with a 95% confidence interval of ±0.1 s. The effect of grid resolution on the observed oscillatory behavior is illustrated in Fig. 3. The oscillation period was 4.7 ± 0.2 s for all the cases; so, the result is not an artifact of insufficient grid resolution. Similarly, the initial conditions did not play any detectable role on the final oscillatory state reached in the simulations.

Fig. 4 shows the effect of grid resolution for a quasi-1D simulation corresponding to the same condition as in Fig. 3; a relatively coarse simulation with only 20 lateral grids yielded an oscillation period of ~ 4.5 s, while those with 40, 80 and 160 lateral grids gave oscillation periods of 4.7 ± 0.2 s, which was the same as the estimated period for 2D simulations (in Fig. 3). As quasi-1D simulations are much faster, we performed a large number of such simulations to explore the effects of various physical parameters on the oscillation period, while ensuring that grid-independent estimates for the oscillation period was obtained in every case.

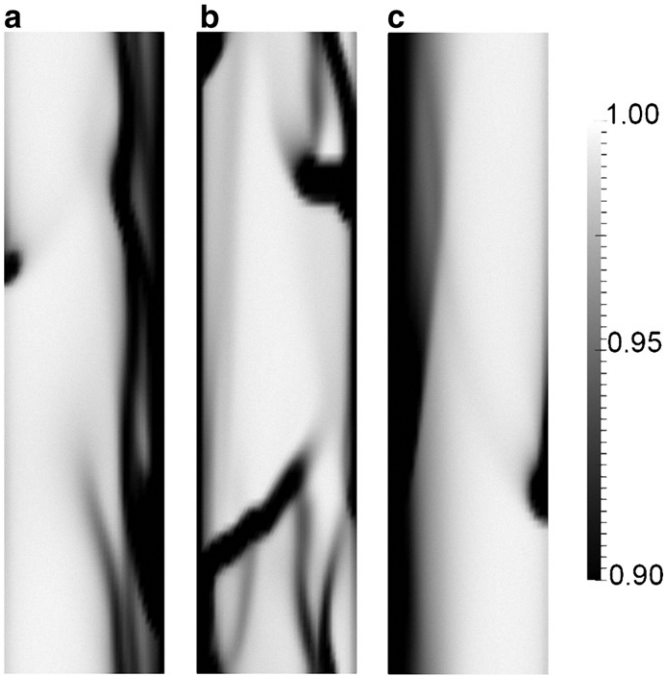

Fig. 1. Gray-scale plots of gas volume fraction field at three successive times within the statistic steady state. Simulation was performed in a 0.10 m × 0.40 m 2-D vertical channel. Channel width = 0.10 m. Height = 0.40 m. Periodic boundary condition was imposed in the axial direction. Average upward gas flux = 6.5 kg/m^{2}s.Domain-average solid volume fraction = 0.05, 40 × 80 grids. Physical properties used in the simulations are listed in Table 1.

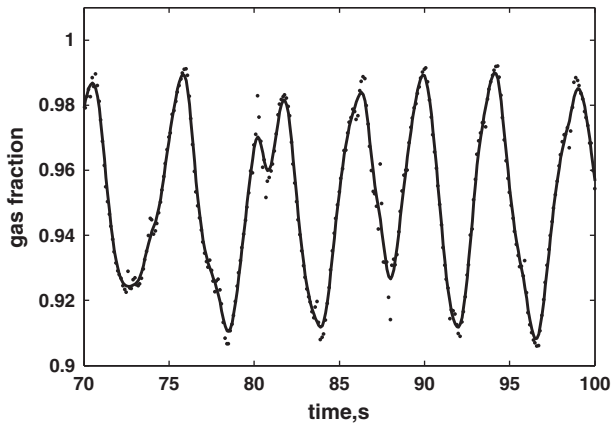

Fig. 2. Variation of average volume fraction of gas in one half of the 2-D channel with time. Symbols indicate the results extracted from simulation. Line is drawn to guide the eye. Simulation conditions are as in Fig. 1.

Based on dimensional analysis, we write

$$\frac{\tau v_t}{W} = h\left(\frac{u_g}{v_t}, \frac{v_t^2}{gd_p}, \frac{v_t^2}{gW}, \langle\phi_s\rangle, \varphi, e_{pp}, e_{pw}\right) \tag{5}$$

and the *dimensional* physical parameters were varied in a systematic manner so that each of the *dimensionless* parameters was varied one at a time while the others were kept constant. The range of dimensional parameters considered in our simulations is summarized in Table 2. These simulations revealed that the oscillation period made dimensionless as in Eq. (5) depends primarily on particle Froude number, $Fr_p = \frac{v_t^2}{gd_p}$ (see Fig. 5a) and domain-average solids volume fraction, $\langle\phi_s\rangle$ (see Fig. 5b). Other quantities on the right hand side of Eq. (5) had only a weak effect on the dimensionless oscillation period. The results in Fig. 5a and b can be captured as

$$\frac{\tau v_t}{W} = 10 Fr_p^{1/2} \cdot \langle\phi_s\rangle^{1/2}. \tag{6}$$

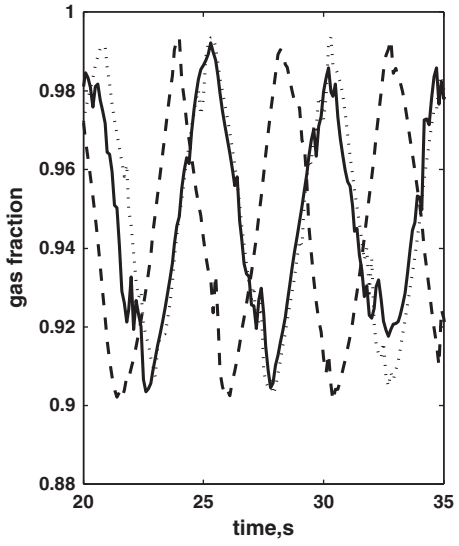

Fig. 3. Effect of grid resolution on the temporal variation of the average volume fraction of gas in one half of the 2-D channel. Simulation conditions are as in Fig. 1. Grid resolution: 40 × 20 (dashed line); 40 × 40 (dotted line); and 40 × 80 (solid line).

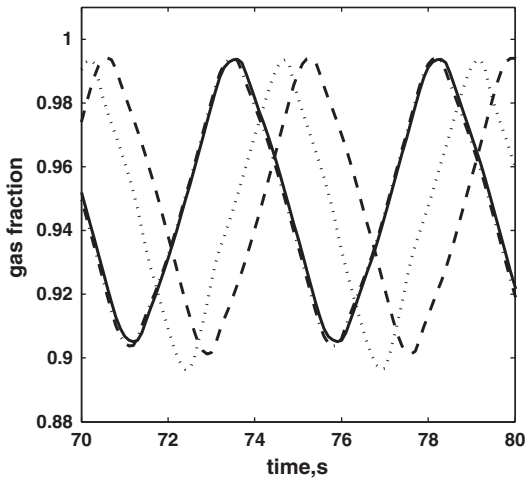

Fig. 4. Effect of grid resolution on the temporal variation of the average volume fraction of gas in one half of the 2-D channel. Simulation conditions are as in Fig. 3, except that we now have a single grid in the axial direction, so that it is in effect a quasi-1D simulation where all quantities depend only on lateral coordinate and time. Grid resolution: 20 × 1(dotted line); 40 × 1 (dashed line); 80 × 1(dash-dotted line); 160 × 1(solid line).

This can further be simplified as

$$\tau = 10\frac{W\langle\phi_s\rangle^{1/2}}{\sqrt{gd_p}}. \tag{7}$$

If the vertical walls were replaced with periodic boundary conditions, we found that similar structure (as in wall-bounded systems) formed and traveled laterally. However, as there were no walls now to reflect the laterally traveling wave, the wave simply kept traveling on the same direction. The initial condition determined whether one obtained left- or right-traveling waves. It is therefore reasonable to surmise that the occurrence of the laterally traveling wave has a microscopic origin and is not driven by the presence of the walls per se; in other words, they derive from the two-fluid model equations and not the boundary conditions.

Note that the oscillation period in Eq. (7) is proportional to the channel width; this implies that the speed with which the laterally traveling wave travels is independent of the channel width, but is proportional to a *particle-scale* characteristic velocity $\sqrt{gd_p}$. This further reinforces the argument that the waves have a microscopic origin embodied in the two-fluid model.

The aspect ratio (L/W) of the periodic domain does not appear as a parameter in Eq. (5) as only one grid was considered in the vertical direction. We therefore set out to see how L/W affects the oscillation period by performing 2D simulations with L/W of 4, 8 and 12. It was found that while the width W was important (see Eq. (7)), L/W had only a weak influence on the oscillation period (over the range of L/W values investigated). As one would expect, at large aspect ratios, the flow patterns developed some axial structure and the columnar structure got more and more distorted. Nevertheless, a quasi-periodic flow structure such as that shown in Fig. 2 persisted robustly in our simulations.

Table 1
Physical properties of gas and solids for the base case.

2-D geometry size	W = 0.1 m, L = 0.4 m	3-D geometry size	D = 0.1 m, H = 0.4 m
ρ_g	1.3 kg/m^3	g	9.81 m/s^2
μ_g	1.8×10^{-5} kg/m s	ϕ_{max}	0.56
ρ_S	2400 kg/m^3	φ	0.0001
d_p	2.0×10^{-4} m	e_{pw}	0.7
$\langle\phi_s\rangle$	0.05	e_{pp}	0.95
m	6.5 kg/m^{2}s		

Table 2
Studied ranges of parameters in "quasi-1D"simulations.

W	0.01–0.3 m	$\langle\phi_s\rangle$	0.05–0.40
ρ_S	1500–3600 kg/m^3	φ	0.0001–0.1
d_p	75–300 μm	e_{pw}	0.3–0.9
m	4–10 kg/m^{2}s	e_{pp}	0.9–0.98

The sensitivity of the results to wall boundary conditions was also investigated. It was found that the boundary condition for the gas phase had no influence on the oscillation period. In contrast, the wall boundary conditions for the particle phase had a substantial effect. Free-slip boundary conditions for the particles produced essentially the same oscillation period as the partial slip boundary condition (with base case values for the particle-wall restitution coefficient and specularity coefficient); however, when no-slip boundary condition was imposed for the particle phase, the oscillations disappeared. Thus, it is reasonable to conclude that the boundary conditions determine whether the laterally traveling wave is reflected or completely annihilated.

The kinetic theory closure was found to be essential to generate the oscillations. When we replaced the kinetic theory model for particle phase pressure and viscosity by simple expressions of the form:

$$p_s = A_1\rho_s v_t^2\phi_s g_o(\phi_s); \mu_s = A_2\rho_s v_t d_p\phi_s g_o(\phi_s) \quad (8)$$

where $g_o(\phi_s)$ is the radial distribution at contact, and A_1 and A_2 are adjustable parameters (assigned values between 0.01 and 1.0), the oscillations disappeared. Thus, the granular energy equation and the kinetic theory closure played an important role in inducing the oscillations. It should be remarked that the average oscillation period

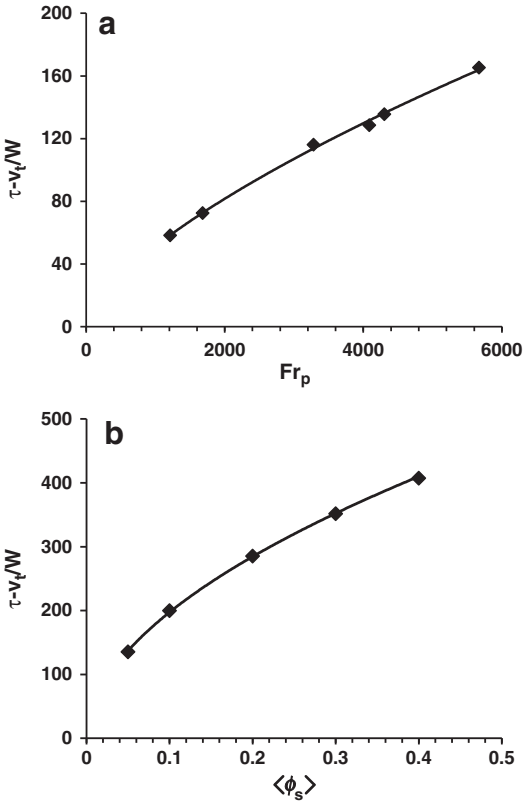

Fig. 5. Dependence of scaled oscillation period on (a) particle Froude number, Fr_p and (b) the domain-average solid volume fraction, $\langle\phi_s\rangle$.Symbols: results from quasi-1D simulations. Lines are drawn to guide the eye. The basic simulation setup is as in the caption of Fig. 4. In panel (a), Fr_p was varied by changing v_t and d_p while the domain-average solid volume fraction was kept constant at 0.05. In panel (b), $\langle\phi_s\rangle$ was varied while particle Froude number, Fr_p, was fixed at 4300.

decreased slightly with increasing particle–particle coefficient of restitution. For example, for the base case, the periods of oscillation were 4.9 s, 4.67 s and 4.35 s for particle–particle coefficients of restitution (e_{pp}) of 0.92, 0.95, 0.98, respectively. Thus, strictly speaking, Eq. (7) is incomplete and it should include a dependence on particle–particle coefficient of restitution; however, this dependence is deemed relatively weak.

It is interesting to ask why the inclusion of granular energy equation induces this character. It is well known that homogeneously fluidized state in gas-particle systems gives way to instabilities that take the form of traveling waves. When phenomenological closures of the type given in Eq. (8) are employed, the most unstable mode is a vertically traveling wave having no horizontal structure [24,25], and purely transverse disturbances are not amplified. In contrast, when kinetic theory closures are introduced, the fluidized state is predicted by unstable to transverse disturbances as well [26,27].

3.2. Flows in vertical cylinders

Fig. 6 shows gray-scale plots of gas volume fraction field at three successive times within the statistic steady state obtained in a 3D simulation of flow in a 0.10 m diameter riser. Periodic boundary condition was applied in the axial direction and the gas mass flux was held fixed at 6.5 kg/m^2.s. The simulation domain was discretized using Cartesian *cut cells* [28]; it was ascertained that similar results were obtained even if we employed cylindrical polar coordinates (not shown). It is clear from Fig. 6 that a particle-rich region is slowly spinning around in the simulation domain. This structure had almost no axial variation, so that it is essentially columnar. (The oscillating wave structure seen in 2D channel flow simulations is replaced by a spinning mode in 3D cylindrical flow simulations.) The average volume fraction of gas in a thin strip running from the axis to the tube wall, over the entire height of the domain and one grid cell thick is presented as a function of time in Fig. 7. Quasi-periodic oscillations are clearly evident. The period of revolution was found to be ~ 3.2 ± 0.3 sec. Essentially the same results were obtained in quasi-2D simulations (containing only one grid in the axial direction) as well; this is consistent with what we observed in channel flow simulations.

As the aspect ratio of the simulation domain was increased, some axial structure became visible, suggesting a transition from *spinning* flow (with little axial structure) to *swirling* flow (with some axial structure). Fig. 8 shows a snapshot of swirling flow structure for typical fluid catalytic cracking particles. In our simulations, the swirling flow structure was observed intermittently only when the axial length of the simulation domain was considerably longer than the product of the period of revolution of the spinning flow structure and the average velocity of particles in the domain.

As in channel flow simulations, we examined the effect of various (physical) parameter values on the period of revolution in 3D as well as quasi-2D cylindrical riser flows. No-slip boundary conditions for the particle phase eliminated the spinning motion, but such motion persisted with free or partial slip boundary conditions for the particles. The boundary condition for the gas had no measurable effect.

Simulation results show that the swirling behavior in 3D risers has the same dependency with the oscillatory behavior happened in 2D channel simulations. Like 2D simulation results, the only way to stop the swirling is the application of no-slip wall boundary condition for particle phase. In Fig. 9, we have plotted the period of oscillation in channel flow and revolution in cylindrical riser flow against the functional group identified previously (see Eq. (7)). R in the abscissa refers to tube radius for cylindrical riser and channel width W for channel flows. It is remarkable that the same characteristic time, $R\langle\phi_s\rangle^{1/2}/\sqrt{gd_p}$ applies to both systems. This further suggests that the same particle scale mechanism is operative in both cases.

As noted above, the period if the spinning (or swirling) motion is of the order of a few seconds. Thus, in most risers, one is likely to see

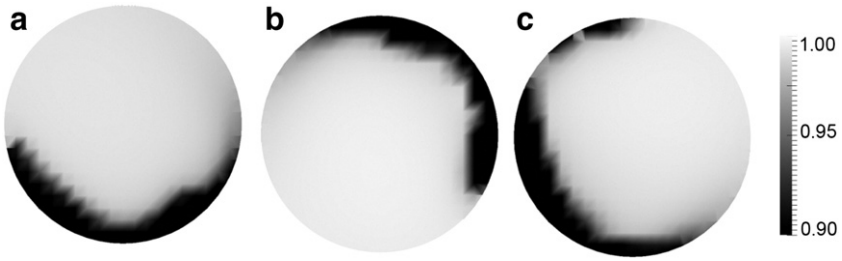

Fig. 6. Snapshots of the gas volume fraction field extracted at three successive times within the statistic steady state. 3-D simulation was performed in a vertical cylinder. Diameter = 0.10 m. Height = 0.40 m. Periodic boundary condition was imposed in the axial direction. Average upward gas flux = 6.5 kg/m^{2}s. Domain-average solid volume fraction = 0.05. Physical properties used in the simulations are listed in Table 1. Cartesian *cut cells* [28] were used in the horizontal plane. 20 grids were placed in vertical direction; the length of the grid in the lateral plane is ~5% of the tube diameter.

at most one spin or swirl as the particles travel from the bottom to the top. Even though this spinning motion is slow compared to the axial velocity, the resulting centrifugal force on the particles may enhance the segregation of particles towards the wall; to assess this effect, we examined the extent of radial segregation of particles in a quasi-2D simulation of flow in a cylindrical riser during flow development. Initially a spinning flow set in with a slow spinning rate, which gradually increases towards the final value. The radial profiles of particle volume fraction at different times (corresponding to different spinning periods) are presented in Fig. 10. It is clear that the extent of segregation is larger at lower spin periods (corresponding to faster spins). Thus, organized azimuthal motion in risers may play a role in establishing radial segregation of profiles; axisymmetric cylindrical flow simulations of riser flow would completely miss this path towards segregation and may lead to both over-estimation of flow development length and under-estimation of extent of segregation.

Assuming that a spinning flow structure with a spin rate as given in Fig. 10 has been established, one can estimate how long it would take a particle to segregate from the center to the wall region. Such an analysis suggests a segregation time: $t_{seg} = \frac{5\sqrt{2}}{\pi}\frac{R\langle\phi_s\rangle^{1/2}}{\sqrt{gd_p}}$. This suggests segregation times of ~1 s and ~10 s for 0.1 m and 1.0 m diameter risers. If the average residence time of the particles in the riser is of this order of magnitude, spinning flow may play a role in establishing and enhancing radial segregation. If the nature of the inlet geometry is such that it promotes spinning motion (e.g., by forming rope-like structures that can quickly develop a spin, as is common in cyclone separators and pneumatic conveying through elbows), then the segregation time will be even less.

4. Summary

Quasi-1D simulations of kinetic theory based two-fluid models for gas-particle flows in vertical channels by Benyahia et al. [13,14] resulted in quasi-periodic flow structures. In the present study, we have performed many 2D simulations of flows in vertical channel segments and 3D simulations of flows in vertical cylindrical segments, and supplemented them with simpler quasi-1D (for channel flow) and quasi-2D (for cylindrical geometry) simulations. Oscillatory flow was observed robustly in 2D and quasi-1D channel flow simulations; spinning flow structures resulted in 3D and quasi-2D simulations of flows in cylindrical geometries. The period of such flow structures could be correlated using a simple model, according to which the speed associated with these structures scales as $\sqrt{gd_p/\langle\phi_s\rangle}$. This, in turn, suggests an instability mode contained in the kinetic theory based two-fluid model as the driver for these

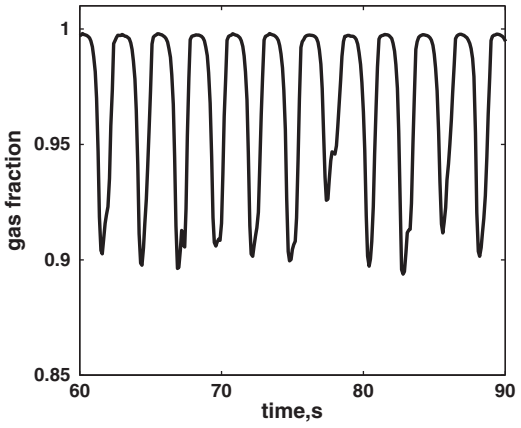

Fig. 7. Variation of average volume fraction of gas in a thin strip in the 3-D cylindrical riser as a function of time. Symbols indicate the results extracted from simulation. Line is drawn to guide the eye. Simulation conditions are as in Fig. 6. The thin strip runs from the axis to the tube wall, over the entire height of the domain and one grid cell thick.

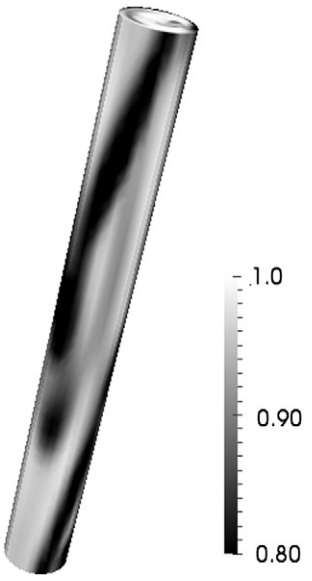

Fig. 8. Snapshot of the gas volume fraction field in the statistic steady state for flow in a long 3-D vertical cylinder, illustrating spiral flow. Diameter = 0.10 m. Height = 0.80 m. Periodic boundary condition was imposed in the axial direction. Average upward gas flux = 0.68 kg/m^{2}s. Domain-average solid volume fraction = 0.05. Simulations were performed using cylindrical coordinate systems: 15 radial grids; 30 azimuthal grids; 40 axial grids (with uniform Δr, $\Delta\theta$ and Δz). Particle density = 1500 kg/m^3. Particle diameter = 75 μm.

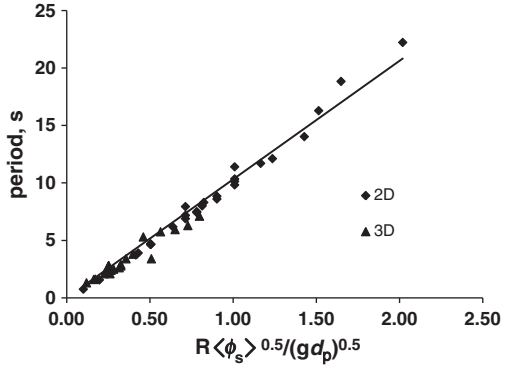

Fig. 9. Oscillation period scales with a characteristic time associated with the system. Only one grid was used in the axial direction in these simulations. For channel flows, R in the figure denotes channel width W. For flows in cylindrical risers, R denotes the tube radius. Simulations covered a wide range of particle Froude numbers and domain-average solid volume fractions, see Fig. 5.

flows. It appears that the observed spinning flow can affect the evolution and extent of radial segregation of particles in gas-particle flows in slender risers.

Notation

A_1,A_2	adjustable parameters in Eq. (8)
d_p	particle diameter, m
e	restitution coefficient
D	cylinder diameter, m
f	drag force per unit volume in two fluid model, kg/m^2.s^2
Fr_p	particle Froude number
g	gravitational acceleration, m/s^2
g_0	radial distribution function at contact in kinetic theory
h	function name in Eq. (5)
H	height of the cylindrical segment, m
J_{coll}	rate of dissipation of granular energy per unit volume through collisions, kg/m.s^3
J_{vis}	rate of dissipation of granular energy per unit volume due to gas, kg/m.s^3
L	height of the channel segment, m
m	gas mass flux, kg/m^{2}s
p	pressure, Pa
q	flux of granular energy, kg/s^3
t	time, s
T	granular temperature, m^2/s^2
u,v	gas and particle phase velocities, respectively, m/s
v_t	terminal settling velocity, m/s
W	channel width, m

Greek letters

Δ	grid size, m
ϕ	volume fraction
$\langle\phi_s\rangle$	domain-average volume fraction
φ	specularity coefficient
λ	granular thermal conductivity, kg/m.s
μ	viscosity, kg/m s
ρ	density, kg/m^3
$\boldsymbol{\sigma}$	stress tensors in two fluid model, kg/m.s^2
τ	period, s
Γ_{slip}	rate of generation of granular energy per unit volume by gas-particle slip, kg/m.s^3

Subscripts

g	gas phase
p	particle
pp	particle–particle
pw	particle–wall
s	particle phase

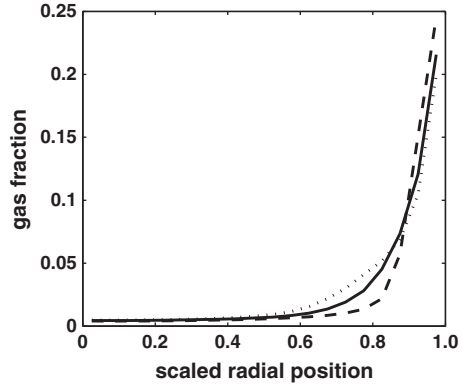

Fig. 10. Radial variation of time-averaged particle volume fraction for different swirling speeds. Results were obtained from a 3-D cylindrical simulation. The swirl rate was initially slow, but became progressively faster. Swirl periods: 3 s (dotted line); 2.2 s (solid line); 1.4 s (dashed line).

Acknowledgments

SS acknowledges the financial support for this work from ExxonMobil Research & Engineering Co. XY acknowledges support from National Basic Research Program of China (2012CB214900) and China Scholarship Council, which allowed her to spend a year at Princeton University. The authors thank Sofiane Benyahia for his assistance with the use of the cut-cell method in this study.

References

[1] J.A. Pita, S. Sundaresan, Developing flow of a gas-particle mixture in a vertical riser, AICHE Journal 39 (1993) 541–552.
[2] J.L. Sinclair, R. Jackson, Gas-particle flow in a vertical pipe with particle–particle interactions, AICHE Journal 35 (1989) 1473–1486.
[3] J. Ding, D. Gidaspow, A bubbling fluidization model using kinetic theory of granular flow, AICHE Journal 36 (1990) 523–538.
[4] A. Neri, D. Gidaspow, Riser hydrodynamics: simulation using kinetic theory, AICHE Journal 46 (2000) 52–67.
[5] J.-F. Parmentier, O. Simonin, O. Delsart, A functional subgrid drift velocity model for filtered drag prediction in dense fluidized bed, AICHE Journal 58 (2012) 1084–1098.
[6] K. Hong, W. Wang, Q. Zhou, J. Wang, J. Li, An EMMS-based multi-fluid model (EFM) for heterogeneous gas–solid riser flows: Part I. Formulation of structure-dependent conservation equations, Chemical Engineering Science 75 (2012) 376–389.
[7] Y. Igci, S. Sundaresan, Verification of filtered two-fluid models for gas-particle flows in risers, AICHE Journal 57 (2011) 2691–2707.
[8] Y. Igci, S. Sundaresan, Constitutive models for filtered two-fluid models of fluidized gas–particle flows, Industrial and Engineering Chemistry Research 50 (2011) 13190–13201.
[9] K. Agrawal, P.N. Loezos, M. Syamlal, S. Sundaresan, The role of meso-scale structures in rapid gas–solid flows, Journal of Fluid Mechanics 445 (2001) 151–185.
[10] A.T. Andrews IV, P.N. Loezos, S. Sundaresan, Coarse-grid simulation of gas-particle flows in vertical risers, Industrial and Engineering Chemistry Research 44 (2005) 6022–6037.
[11] Y. Igci, A.T. Andrews, S. Sundaresan, S. Pannala, T. O'Brien, Filtered two-fluid models for fluidized gas-particle suspensions, AICHE Journal 54 (2008) 1431–1448.
[12] C.C. Milioli, F.E. Milioli, W. Holloway, K. Agrawal, S. Sundaresan, Filtered two-fluid models of fluidized gas particle flows: new constitutive models, AIChE Journal (unpublished results).
[13] S. Benyahia, A time-averaged model for gas–solids flow in a one-dimensional vertical channel, Chemical Engineering Science 63 (2008) 2536–2547.
[14] S. Benyahia, M. Syamlal, T.J. O'Brien, Study of the ability of multiphase continuum models to predict core-annulus flow, AICHE Journal 53 (2007) 2549–2568.
[15] P.R. Naren, V.V. Ranade, Scaling laws for gas–solid riser flow through two-fluid model simulation, Particuology 9 (2011) 121–129.
[16] S. Benyahia, M. Syamlal, O.B. TJ, Consistency of fully developed and periodic simulations in gas/solids flow in a riser, AIChE Annual Meeting, Cincinnati, OH, 2005.

[17] D. Gidaspow, Multiphase Flow and Fluidization, Academic Press, CA, 1994.
[18] R. Jackson, The Dynamics of Fluidized Particles, Cambridge University Press, UK, 2000.
[19] M. Syamlal, MFIX Documentation:Numerical Techniques, DOE/MC-31346-5824, 1998.
[20] M. Syamlal, W. Rodgers, T. O'Brien, MFIX Documentation theory guide, DOE/METC-94/1004, 1993.
[21] M. Syamlal, W. Rodgers, T. O'Brien, MFIX documentation, U.S. Department of Energy, Federal Energy Technology Center, Morgantown, WV, 1993.
[22] C.Y. Wen, Y.H. Yu, Mechanics of fluidization, Chemical Engineering Progress Symposium Series 62 (1966) 100–111.
[23] P.C. Johnson, R. Jackson, Frictional-collisional constitutive relations for granular materials, with application to plane shearing, Journal of Fluid Mechanics 176 (1987) 67–93.
[24] B.J. Glasser, I.G. Kevrekidis, S. Sundaresan, Fully developed travelling wave solutions and bubble formation in fluidized beds, Journal of Fluid Mechanics 334 (1997) 157–188.
[25] B.J. Glasser, S. Sundaresan, I.G. Kevrekidis, From bubbles to clusters in fluidized beds, Physical Review Letters 81 (1998) 1849–1852.
[26] A.K. Didwania, A new instability mode in fluidized beds, Europhysics Letters 53 (2001) 478–482.
[27] K. Mandich, R.J. Cattolica, Longitudinal and transverse disturbances in unbounded, gas-fluidized beds, Physics of Fluids 25 (023301) (2013) 1–18.
[28] J. Dietiker, Multiphase flow with interphase eXchanges: Cartesian grid user guide, 2012.